A. Théron
Département de Mécanique et Technologie,
Commissariat à l'Énergie Atomique,
Saclay, 91191 Gif-sur-Yvette, France

E. de Langre[1]
LadHyX, CNRS,
École Polytechnique,
91128 Palaiseau, France
Mem. ASME

C. Putot
Institut Français du Pétrole,
92852 Rueil-Malmaison, France

The Effect of Dynamical Parameters on Precession in Rotary Drilling

Precession, which is the rolling motion of the drillstring on the walls of the borehole, is investigated by considering the various possible motions of a rotating disk in a circular hole. Due to the simplicity of the model, closed-form results are derived on the stability of precession and on the evolution of impacting motions towards precession. It is found that increasing coefficients of friction and contact damping have a favoring effect on precession, while the stiffness and damping of the drillstring bending mode have an opposing effect. [DOI: 10.1115/1.1383974]

1 Introduction

In the process of oil well drilling, vibrations of drillstrings are often experienced and may lead to poor efficiency of the process, excessive wear of tools, or fracture of the drilling system. It may be easily understood that a drilling system of the vertical rotary type is naturally prone to vibrations. It consists of a drilling tool which cuts off the rock, a set of heavy tubes of a lesser diameter to apply a compressive load on the tool, and thinner tubes that transmit the rotational torque from the surface. It should be noted that in normal drilling conditions part of the lower part of the drill string, or bottom-hole assembly (BHA), is under axial compression, while the upper tubes are under tension.

Though actual motions of the drillstring have only been recently measured [1–3], it is a common feature to distinguish between vertical and lateral vibrations, even if some coupling may exist [4]. Vertical vibrations are more specifically related to the interaction of the tool with the rock and occasional ''bit-bouncing'' effects. As they are well transmitted all along the drillstring, their monitoring and control from the surface operators is now part of the know-how of oil-well drilling.

The case of lateral vibrations is somewhat different and will be the main concern of the present paper. Such motions are not easily transmitted along the drillstring, as flexural waves are more sensitive to fluid damping and dispersion of energy. While rotating in the borehole, the shaft may experience local sideways vibrations with or without impact on the wall, or even precession, which is continuous contact with orbital rolling or sliding on the borehole. The sideway impacts may be the source of sharp impulses of stress, but precession is actually the most damaging motion. In fact, the whirl on the borehole, Fig. 1, may result in high alternative bending stress and consecutive fatigue [5] or abrasive wear of the wall. Aldred and Sheppard [2] pointed out that contact with the borehole is the main source of energy transmission from the rotary motion to transverse vibrations.

From a practical point of view, there is actually a need to relate the existence of precession to operating parameters such as the rate of rotation of the drillstring, its bending characteristics, or the physics of the contact with the borehole, which depend on the rock and fluid environment. It is also needed to determine the influence of these parameters on the possibility that vibrations with impacts may degenerate into precession.

Jansen [6] analyzed the conditions of lateral stability of the shaft, assuming permanent contact between the borehole and the stabilizer. Depending on the values of gaps and friction coefficient, criteria were proposed for the stability of forward or backward whirl. Numerical models have also been used [7], assuming nonlinear impact interactions of the vibrating BHA with the borehole. Experimental simulations of such systems have pointed out the large variety of vibrationnal instabilities that may arise [8]. Though such models allow a close representation of geometrical and physical hypothesis, the understanding of the mechanisms that actually control the occurrence of precession is not easy.

In that sense, the present paper will be focused on analytical aspects of the stability of the various aforementioned motions. More specifically, we will analyze the conditions under which lateral vibrations with impacts degenerate into stable precessions. The simplified model of the dynamics of the BHA is described in Section 2. In Section 3, the evolution from occasional impacts with the borehole to precession is considered. The stability of this precession is analyzed in Section 4.

2 Simplified Mechanical Model

To emphasize the effect of mechanical parameters, closed-form results are sought for the various aforementioned phenomena. In that sense, a simple model of the BHA is considered here, which does not have a strong quantitative relevance, but is expected to capture most of the basic phenomena that control precession. The

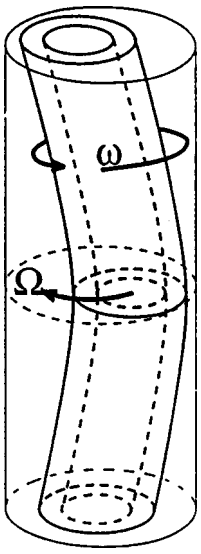

Fig. 1 Precession of a rotating drillstring

[1]Corresponding author.

Contributed by the Petroleum Division for publication in the JOURNAL OF ENERGY RESOURCES TECHNOLOGY. Manuscript received by the Petroleum Division, June 10, 1999; revised manuscript received April 10, 2001. Editor: A. K. Wojtanowicz.

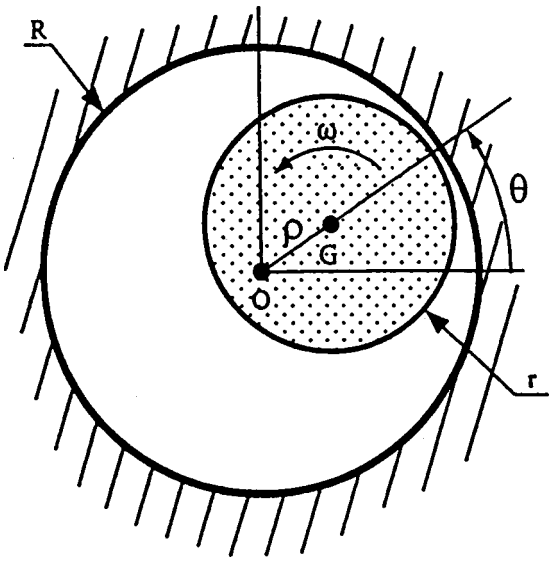

Fig. 2 Simplified mechanical model

BHA is modeled as a rotating rigid disk, of radius r and mass M moving in a circular hole of radius R center at point O, Fig. 2, as in [6,9]. The elastic bending of the shaft is taken into account through two orthogonal modes of vibration frequency ω_B and reduced damping ξ. The rate of rotation of the disk, ω, is not affected by the contact with the hole due to the large torsional stiffness and rotating inertia of the drilling system. In polar coordinates $\rho(t)$ and $\theta(t)$, the equations of motion of the center of the disk read

$$M(\ddot{\rho}-\rho\dot{\theta}^2)+2\xi\omega_B M\dot{\rho}+M\omega_B^2\rho=F_\rho \tag{1}$$

$$M(\rho\ddot{\theta}+2\dot{\rho}\dot{\theta})+2\xi\omega_B M\rho\dot{\theta}=F_\theta \tag{2}$$

where F_ρ and F_θ are external forces exerted on the disk, and $(\dot{})$ denotes the time derivative. Note here that F_θ is positive in the clockwise direction. In our model, these external forces will only consist of the impact and friction forces described in the forthcoming. Fluid-induced forces are taken into account in the parameters M, ω_B, ξ and in the impact parameters.

The radial restoring force that models contact with the borehole is defined by an elastic stiffness K and a damping coefficient η and reads

$$F_\rho=-K[\rho-(R-r)]-2\eta\dot{\rho}\sqrt{MK} \tag{3}$$

when $\rho>R-r$ and is zero otherwise. The tangential force follows Coulomb's law of friction, which includes the possibility of sliding or adherence.

$$\text{Sliding: } F_\theta=\mu F_\rho \quad \text{and} \quad \dot{\theta}\neq-\omega r/(R-r) \tag{4}$$

$$\text{Adherence: } F_\theta<\mu F_\rho \quad \text{and} \quad \dot{\theta}=-\omega r/(R-r) \tag{5}$$

In this simple model, we shall use the same coefficient of friction in (4) and (5), though differences are known to exist and have an influence on phenomena such as stick-slip instabilities.

3 Evolution Towards Precession

In this section, we shall consider the conditions under which the motion of the rotating BHA, in our model, may progressively shift from a succession of impacts to precession, which is constant rolling or sliding contact. Two elementary models are described further, one for the impact which will give a "law of impact," Eqs. (8) to (10), and one for the flight between two impacts which will give a "law of flight," Eq. (11) and Appendix B.

Impacts are assumed to be of a short duration compared to the period of motion of the BHA in the borehole, so that they may be modeled as the impacts of a rotating disk on a flat plane, Fig. 3. The motion in relation with the plane of impact is defined by the normal and tangential velocities, V_n and V_t. For the sake of simplicity, the normal velocity is always counted as positive. Let us define the dimensionless velocities

$$u=\frac{V_n}{r\omega}, \quad v=-\frac{V_t}{r\omega} \tag{6}$$

The equations of motion (1) and (2) may be explicitly integrated in the case of planar impact, Appendix A, to derive the velocities at the end of contact (u^+,v^+) as functions of those before impact (u^-,v^-). The normal velocity is expressed as $u^+=Xu^-$ where the coefficient of restitution X is given by

$$X=e^{-a\eta[\arctan(2b\eta)+\pi]}, \quad a=1/\sqrt{1-\eta^2}, \quad b=1/[a(2\eta^2-1)] \tag{7}$$

when damping is small enough, $\eta<\sqrt{2}/2$; see [10]. The tangential velocity depends on the existence of sliding or sticking phases during the impact, so that, defining $q=\mu(1+X)u^-$, we have

$$v^+=v^-+q \quad \text{if} \quad v^-<1-q \tag{8}$$

$$v^+=1 \quad \text{if} \quad 1-q<v^-<1+q \tag{9}$$

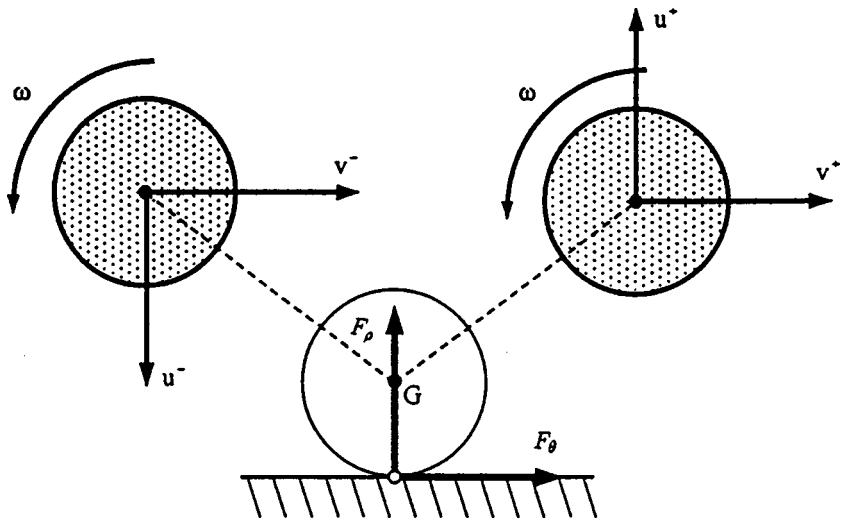

Fig. 3 Model of impact

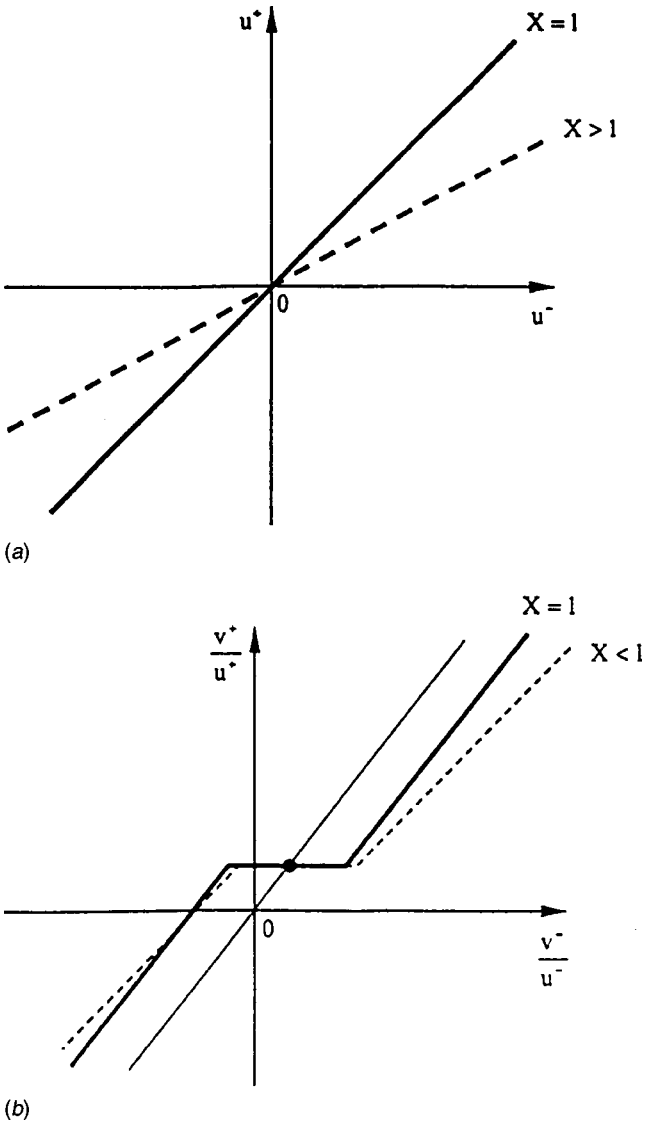

Fig. 4 Law of impact—(*a*) normal velocity after impact as a function of the normal velocity before impact; (*b*) angle of rebound as a function of the angle of impact

$$v^+ = v^- - q \quad \text{if} \quad v^- > 1 + q \tag{10}$$

This approach is different from that of recent papers [4] as the dynamic equations are solved explicitly, thus capturing the transition from bouncing to sliding and adherence, as in [11]. It may be seen in Fig. 4 that the angle of rebound as defined by its tangent v^+/u^+ is larger or smaller than the angle of impact, depending on the respective values of the rate of rotation ω, the coefficient of friction μ, and the impact damping η. This is due to the simultaneous, but independent, evolutions of the normal velocity through impact damping and of the tangential velocity through friction.

Considering now the motion between two impacts, or flight motion, a relation is needed to derive the velocities at the beginning of an impact (u_{p+1}^-, v_{p+1}^-) from those at the end of the previous impact (u_p^+, v_p^+), where p denotes the index of impact. The equations of motion may be integrated in the simple case where the effect of flexural damping ξ is neglected. In that particular case, the law of flight thus reduces to

$$(v_{p+1}^-, u_{p+1}^-) = (v_p^+, u_p^+) \tag{11}$$

The more general case will be discussed in the forthcoming.

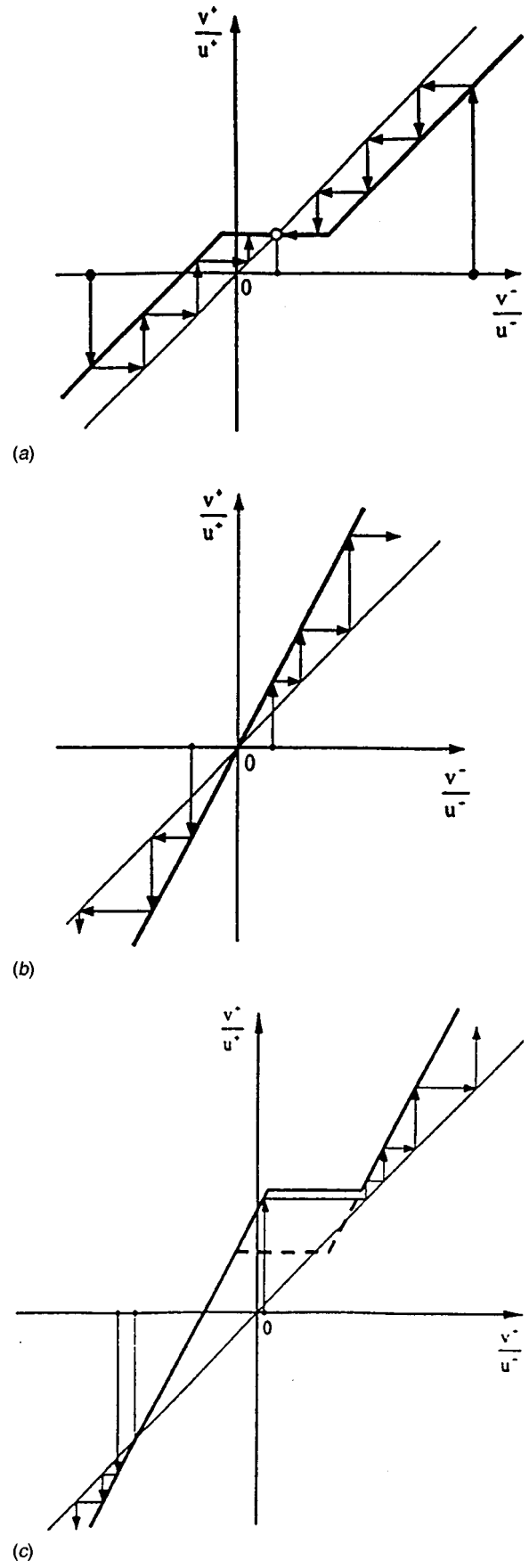

Fig. 5 Evolution from impacting motions to precession—(*a*) friction, but no impact damping; (*b*) impact damping, but no friction; (*c*) general case: friction and impact damping

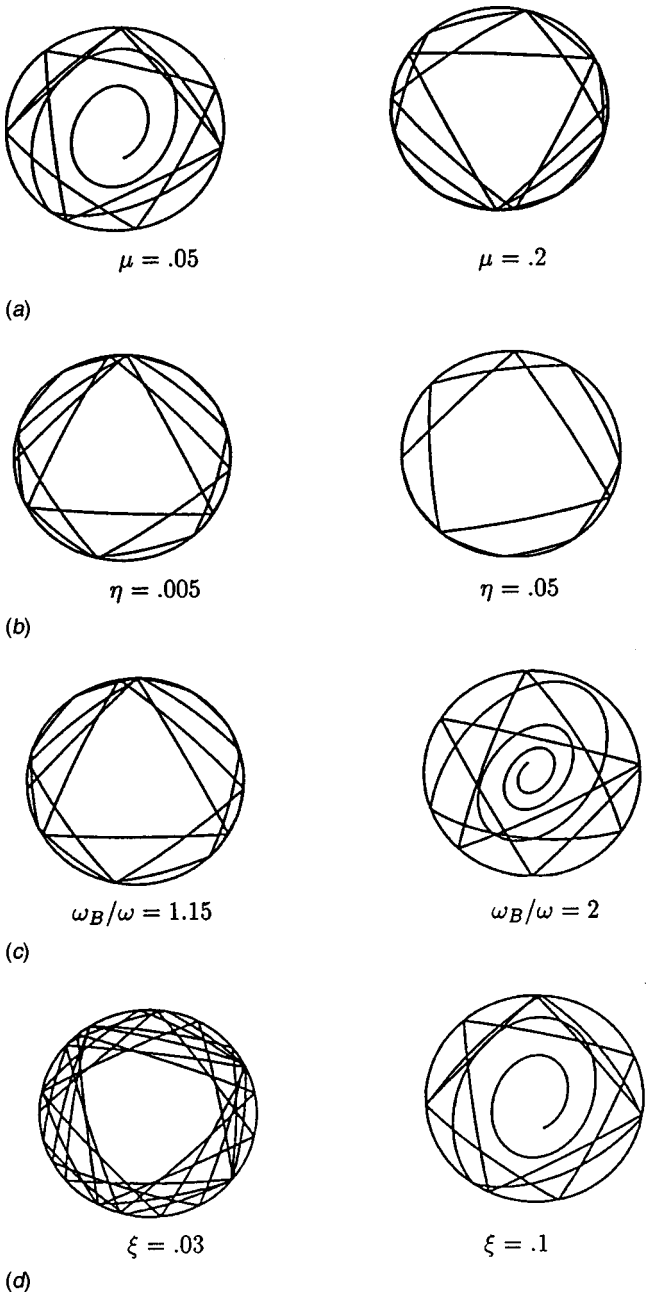

Fig. 6 Effect of mechanical parameters on the trajectory in the borehole. Unless otherwise specified, the parameters are $\mu=.2$, $\eta=.005$, $\omega_B/\omega=1.15$, $\xi=.1$. (*a*) Effect of the coefficient of friction; (*b*) effect of the impact damping coefficient; (*c*) effect of the frequency of bending; (*d*) effect of the flexural damping.

The preceding models of impact and flight may now be combined to study the evolution of successive impacts, and by doing so, to identify limit cycles of the system, if any. This will be done using a simple graphical procedure in the space of rebound angle (u/v), where the value of the rebound angle before and after each impact is iteratively determined by the alternative use of Fig. 4 and Eq. (11). For a given set of initial velocities, say (u_0^-, v_0^-), the velocities after impact (u_0^+, v_0^+) are given by Fig. 4. The components of velocity at the next impact are then given by Eq. (11), so that

$$\frac{v_1^-}{u_1^-}=\frac{v_0^+}{u_0^+} \tag{12}$$

This procedure may be graphically iterated, Fig. 5, and allows to identify the ultimate behavior of the impacting BHA, depending on the initial conditions and the physical parameters. Precession is the case where the angle of impact is $\pm\pi/2$, which is $(v/u)\rightarrow\pm\infty$.

Three different cases arise: if $\mu\neq 0$, but $\eta=0$, any motion tends towards a succession of impacts with constant angle, Fig. 5(*a*), the value of which only depends on the initial normal velocity and the rate of rotation

$$\frac{v}{u}=\frac{1}{u}=\frac{r\omega}{V_n} \tag{13}$$

This angle is such that $V_t=-r\omega$, which is the condition of rolling without sliding. Conversely, when $\mu=0$, but $\eta\neq 0$, only the normal velocity is affected by the impact and the angle of rebound increases up to a simple orbital motion on the wall, Fig. 5(*b*). In the general case of $\mu\neq 0$, $\eta\neq 0$, the graphical procedure is somewhat modified by the diminution of the normal velocity at every impact, as was shown in Fig. 4(*a*). The plateau in the impact law, Fig. 4(*b*), therefore, progressively moves upwards, ultimately leading again to limit cycles of clockwise or anticlockwise orbital motions, Fig. 5(*c*). From this analysis, it may be concluded that the presence of impact damping induces precession as the final stable or steady state, even if friction and rotation of the shaft are taken into account.

In the most general case where the damping of flexural modes is not negligible, the law of flight is much more complex, as the free trajectory of the disk is an exponential elliptic spiral. Hence, the parameters such as the velocities at the next impact may only be derived through the numerical solution of implicit equations which are derived in Appendix B. It should be noted that in that case, there exists a range of velocities (u_p^+, v_p^+) such that no further impact occurs. Using now alternatively the impact law, Eq. (4), and a numerical solution of the law of flight, the evolution of the motion of the BHA may be computed for any initial conditions. To show the influence of the relevant mechanical parameters on the evolution towards precession, typical results are presented in Fig. 6. Depending on the values of the contact parameters μ, η, and of the BHA parameters ω_B and ξ, the ultimate motion is seen to be either precession or loss of contact.

Clearly, the parameters that induce precession are friction and impact damping, whereas flexural damping and stiffness reduce the tendency to whirl.

4 Stability of Precession

Let us now consider the case of permanent contact between the BHA and the borehole. The motion of the disk is then fully described by the orbital velocity or rate of precession $\Omega(t)$ in Fig. 2. Assuming contact, the equilibrium equations read, using $\dot\theta=\Omega$ and $\dot\rho=\ddot\rho=0$

$$0=F_\rho+M(R-r)\Omega^2-M\omega_B^2(R-r) \tag{14}$$

$$M(R-r)\dot\Omega=F_\theta-2\xi\omega_B M(R-r)\Omega \tag{15}$$

For the sake of clarity, only the case $\Omega>0$ and $\omega<0$ will be considered here, other cases being derived using symmetry. With the dimensionless parameters $\tau=\omega_B t$, $\bar\Omega=\Omega/\omega_B$, $\bar\omega=-r\omega/((R-r)\omega_B)$, $\bar F=F/(K(R-r))$, Eqs. (14) and (15) reduce to

$$0=\bar F_\rho+\bar\Omega^2-1 \tag{16}$$

$$\frac{d\bar\Omega}{d\tau}=\bar F_\theta-2\xi\bar\Omega \tag{17}$$

The law of friction may be expressed now as

$$\bar\Omega=\bar\omega \quad\text{and}\quad \bar F_\theta<\mu\bar F_\rho \tag{18}$$

$$\bar\Omega<\bar\omega \quad\text{and}\quad \bar F_\theta=\mu\bar F_\rho \tag{19}$$

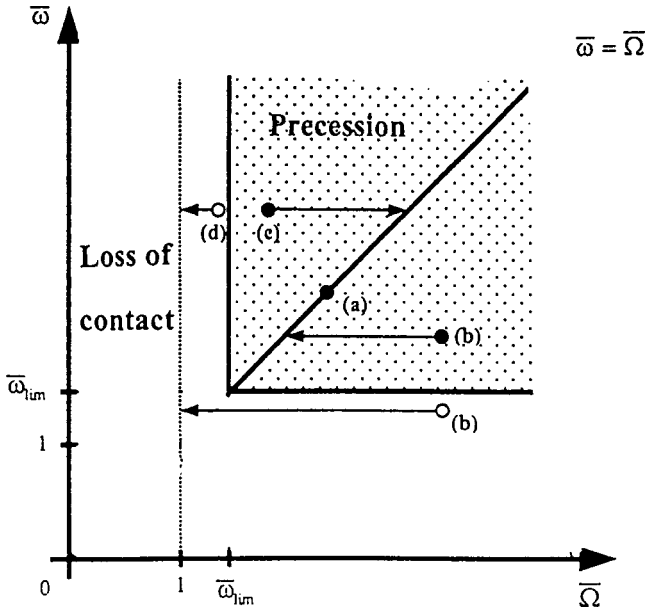

Fig. 7 Evolution of the rate of precession $\overline{\Omega}$ depending on its initial value and on the rate of rotation $\overline{\omega}$: (○) evolution to a loss of contact. (·) evolution to a stable precession. Cases (a), (b), (c). (d) refer to the text.

This set of equations holds only if the contact is effective, that is $\overline{F}_\rho < 0$, or equivalently using Eq. (16) $\overline{\Omega} > 1$, which means the centrifugal force counterbalances the elastic restoring force.

Let us first consider the conditions that allow the rate of precession $\overline{\Omega}$ to remain stationary in time. In that case, Eq. (17) yields $\overline{F}_\theta = 2\xi\overline{\Omega}$. Using Eq. (16), and the law of friction, it is found necessary that the dimensionless rate of rotation exceeds a limit value

$$\overline{\omega} > \overline{\omega}_{\lim} = \frac{\xi}{\mu} + \sqrt{1 + \left(\frac{\xi}{\mu}\right)^2} \tag{20}$$

In dimensional form, this criterion on the rate of rotation reads

$$|\omega| > \omega_B \frac{(R-r)}{r}\left[\frac{\xi}{\mu} + \sqrt{1 + \left(\frac{\xi}{\mu}\right)^2}\right] \tag{21}$$

Hence, the mechanical condition for persisting precession is that the rotational velocity $\overline{\omega}$ is high enough to induce, through friction and the consecutive precession, centrifugal forces that will counterbalance the flexural and damping forces.

If the dependency with time is now included, the set of Eqs. (16)–(19) may be solved for any arbitrary initial rate of precession $\overline{\Omega}(0) = \overline{\Omega}_0$. Four cases appear, as illustrated in Fig. 7: (a) if $\overline{\Omega}_0 = \overline{\omega}$, rolling precession exists, which may hold only if $\overline{\omega} > \overline{\omega}_{\lim}$; (b) if $\overline{\Omega}_0 > \overline{\omega}$, the solution is obtained as

$$\overline{\Omega}(\tau) = \beta\left[\coth\left(\operatorname{acoth}\left(\frac{\overline{\Omega}_0 + \alpha}{\beta}\right) + \beta\tau\right)\right] - \alpha \tag{22}$$

where $\alpha = \xi/\mu$ and $\beta = \sqrt{1+\alpha^2}$, the rate of precession $\overline{\Omega}$ continuously decreases until it reaches $\overline{\omega}$, where rolling precession holds if $\overline{\omega} > \overline{\omega}_{\lim}$ as in the foregoing; (c) if $\overline{\omega}_{\lim} < \overline{\Omega}_0 < \overline{\omega}$, $\overline{\Omega}$ continuously increases as

$$\overline{\Omega}(\tau) = \beta\left[\coth\left(\operatorname{acoth}\left(\frac{\overline{\Omega}_0 - \alpha}{\beta}\right) - \beta\tau\right)\right] + \alpha \tag{23}$$

until it reaches rolling precession, $\overline{\Omega} = \overline{\omega}$, which is stable; (d) if $\overline{\Omega}_0 < \overline{\omega}_{\lim} < \overline{\omega}, \overline{\Omega}$ decreases as

$$\overline{\Omega}(\tau) = \beta\left[\tanh\left(\operatorname{atanh}\left(\frac{\overline{\Omega}_0 - \alpha}{\beta}\right) - \beta\tau\right)\right] + \alpha \tag{24}$$

until it reaches $\overline{\Omega} = 1$, where contact stops. In Fig. 7, it is seen that precession will only result if Eq. (20) is satisfied simultaneously by the rate of rotation $\overline{\omega}$ and by the rate of precession $\overline{\Omega}$.

5 Concluding Remarks

The interaction between a BHA and the wall of the borehole is indeed a complex phenomenon known to be highly nonlinear, and therefore quite unpredictable in its details [2]. Nevertheless, by the use of a simple model, it is thought that some of the relevant physical aspects are captured and that some insight may be given on the laws that govern the existence and stability of some particular motions such as precession. From the analytical results of the preceding sections, one may conclude that:

(a) When a flexible rotating shaft iteratively impacts on the borehole, it ultimately tends to move either in orbital motion, rolling on the wall or is brought back away from the wall by the flexural restoring forces.

(b) Similarly, a rotating shaft may remain in contact with the wall of the borehole only if its rate of rotation is high enough to satisfy a simple criterion, given by Eq. (21). This criterion expresses the influence of damping, friction, and flexural rigidity of the shaft on the stability of precession.

(c) In all these results, it is found that stable precession is enhanced by friction and contact damping, while the bending stiffness and damping have a negative effect.

The results derived in this paper are by nature qualitative due to the simple model considered here. Parameters such as η or M may not be explicitly related to operating drilling parameters. Some relation may nevertheless be made with the analysis of field experiments and with other models. As to the influence of friction on precession, our results are consistent with the analysis of Aldred and Sheppard [2], who compared the motion of a stabilizer in contact with claystone and with sandstone. Higher friction in the latter was found to induce higher level of lateral motion, which led these authors to point out the role of friction-induced tangential forces on lateral impacts of drillstrings. Macpherson et al. [12] observed that increasing the rotary frequency induces higher risks of precession, as in our model. Conclusions derived from other analytical or numerical models, such as in [6] or [9], are also consistent in terms of the effect of friction or rotary frequency. Yet, none of these models show how stable precession is reached as the result of an iterative process of bouncing on walls, as described in Section 3.

Possible further improvements of the present approach are twofold: a different law of friction might be included that would be more applicable to impact and contact in the presence of confined fluid; a model of drilling efficiency such as in [13] would be improved by coupling it with the present model for the lateral motion of the bit.

Nomenclature

F = contact force
K = contact stiffness in model
M = mass of drillstring in model
R = radius of borehole
r = radius of drillstring
V = velocity
u, v = reduced normal and tangential velocities
X = restitution coefficient of contact
t = time
η = contact damping
θ = azimuthal position of disk
μ = coefficient of friction
ξ = damping of bending mode

ρ = radial position of disk
τ = dimensionless time
ω = rate of rotation, vibration frequency
Ω = rate of precession

Subscripts and Superscripts

B = bending mode
lim = limit value
n, t = normal, tangential component
p = index of impact
ρ, θ = radial, azimuthal component
$-, +$ = value before, after impact
$(\bar{\ })$ = dimensionless variable

Appendix A

Derivation of the Law of Impact. The dynamic equations of motion during impact may be solved successively in the normal then tangential directions. In the normal direction, the dimensionless duration of the impact may be derived, which is a half-period of the free motion of the mass M with the stiffness K

$$\tau_I = \sqrt{\frac{K}{M}}\, t_I = \arctan\left(\frac{2\eta\sqrt{1-\eta^2}}{2\eta^2-1}\right) + \pi \tag{25}$$

when damping is small enough, $\eta < \sqrt{2}/2$. In the tangential direction, the friction law makes it necessary to consider the sliding velocity, which is here the tangential velocity at the point of contact, $v_S = (V_T + r\omega)/(-r\omega) = v - 1$. Except in the very particular case where $v^- = 1$, there exists a phase of the impact where the sliding velocity is nonzero. As a result of Coulomb's law of friction, the instantaneous tangential force may be calculated from the instantaneous normal force as $\bar{F}_\theta(t) = \mu \bar{F}_\rho$. Applying this force on the dynamic equation of motion in the tangential direction, the evolution of the tangential velocity may be calculated, as well as that of the sliding velocity. Three cases appear, depending on the value of X, μ, u^-: (a) if $1-\mu(1+X)u^- < v^- < 1+\mu(1+X)u^-$, the sliding velocity comes to zero before the end of impact and the velocity at the end of impact is that of the rolling condition, $v^+ = 1$; (b) if $v^- < 1-\mu(1+X)u^-$, reverse sliding persists during all the duration of impact and the tangential velocity is increased to $v^+ = v^- + \mu(1+X)u^-$; (c) conversely, if $v^- > 1+\mu(1+X)u^-$, forward sliding persists and the BHA is tangentially decelerated so that $v^+ = v^- - \mu(1+X)u^-$.

Appendix B

Derivation of the Law of Free Flight. In the most general case with damping, i.e., $\eta \neq 0$, a condition may be derived on the velocity after rebound, such that another impact will follow. It reads, after integrating the equations of motion (1) and (2) (see [10])

$$(1-X^2-Y^2)\cos Z + 2X\sin Z + (1+X^2+Y^2) - 2e^{\xi(Z+2\pi)} > 0 \tag{26}$$

where $X = u^+\bar{\omega} - \xi$, $Y = v^+\bar{\omega}$, $A = 1+X^2+Y^2-2\xi X$, $B = -X + \xi(X^2+Y^2)$, $Z = 2\arctan[(-B+\sqrt{B^2-4AY})/2A]$. The dimensionless time of free flight, τ_F is then implicitly defined by

$$(1-X^2-Y^2)\cos 2\tau_F + 2X\sin 2\tau_F + (1+X^2+Y^2) - 2e^{\xi 2\tau_F} = 0 \tag{27}$$

and the velocity at the beginning of the next impact by

$$\begin{aligned}(u^-_{p+1}, v^-_{p+1}) = \frac{1}{2}\bar{\omega}e^{-\xi 2\tau_F}([(-2X+\xi(X^2+Y^2-1))]\cos 2\tau_F \\ + (X^2+Y^2-1+2\xi X)\sin 2\tau_F \\ - \xi(X^2+Y^2+1), 2Y)\end{aligned} \tag{28}$$

If Eq. (26) is not satisfied, the BHA permanently leaves contact with the wall of the borehole.

References

[1] Wolf, S. F., Zacksenhouse, M., and Arian, A., 1985, "Field Measurement of Downhole Drillstring Vibrations," *60st Annual Technical Conference and Exhibition of the SPE, Las Vegas, NV*, Paper SPE 14675.
[2] Aldred, W. D., and Sheppard M. C., 1992, "Drillstring Vibrations: A New Generation Mechanism and Control Strategies," *67th Annual Technical Conference and Exhibition of the SPE, Washington*, Paper SPE 24582.
[3] Rey-Fabret, I., Mabile, M. C., and Oudin, N., 1997, "Detecting Whirling Behavior of the Drill String From Surface Measurements," *72nd Annual Technical Conference and Exhibition of the SPE, San Antonio, TX*, Paper SPE 38587.
[4] Yigit, A. S., and Christoforou, A. P., 1998, "Coupled Torsional and Bending Vibrations of Drillstrings Subject to Impact With Friction," J. Sound Vib., **215**, pp. 137–181.
[5] Vandiver, J. K., and Nicholson, J. W., 1990, "Case Studies of the Bending Vibration and Whirling Motion of Drill Collars," SPE Drilling Engineering, **5**, pp. 282–290.
[6] Jansen, J. D., 1991, "Nonlinear Rotor Dynamics as Applied to Oilwell Drillstring Vibrations," J. Sound Vib., **147**, pp. 115–135.
[7] Birades, M., 1986, "Static and Dynamic Three Dimensional Bottomhole Assembly Computer Model," *61st Annual Technical Conference and Exhibition of the SPE, New Orleans, LA*, Paper SPE 15466.
[8] Berlioz, A., Der Hagopian, J., Dufour, R., and Draoui, E., 1996, "Dynamic Modeling of a Drillstring: Experimental Investigation of Lateral Instabilities," ASME J. Vibr. Acoust., **118**, pp. 292–298.
[9] Dunayevsky, V. A., and Abbasian, F., 1995, "Application of Stability Approach to Bit Dynamics," *SPE Annual Technical Conference and Exhibition, Dallas, TX*, Paper SPE 30478.
[10] Théron, A., 1996, "Modélisation des effets non-linéaires de contact dans le processus de forage," PhD thesis, Université d'Evry-Val d'Essonne.
[11] Antunes, J., Axisa, F., Beaufils, B., and Guilbaud, D., 1990, "Coulomb Friction Modeling in Numerical Simulations of Vibration and Wear Work Rate of Multi-Span Heat Exchangers," J. Fluids Struct., **4**, pp. 287–304.
[12] Macpherson, J. D., Jogi, P., and Kingman, J. E., 1998, "Application and Analysis of Simultaneous Near Bit and Surface Dynamics Measurements," *IADC/SPE Drilling Conference, Dallas, TX*, Paper IADC/SPE 39397.
[13] Putot, C. J. M., Perreau, P. J., and Constantinescu, A., 1998, "Field Data vs. Theoretical Model to Quantify Drilling Effiency and Disruption," *SPE European Petroleum Conference, The Hague, The Netherlands*, Paper SPE 50579.